

Table 1.1.
Physical and chemical properties of the alkali metals and the alkaline earths

A. Alkali metals, elements	Li	Na	K	Rb	Cs
Atomic number	3	11	19	37	55
Naturally-occurring isotopes	2	1	3	2	1
Atomic weight (^{12}C)	6.941	22.9898	39.0983	85.4678	132.905
Electron formula	$[\text{He}]2s^a$	$[\text{Ne}]3s^a$	$[\text{Ar}]4s^a$	$[\text{Kr}]5s^a$	$[\text{Xe}]6s^a$
Ionic radius (Å) and coordination number ^a	0.68 (4) 0.82 (6)	1.10 (6) 1.24 (8)	1.59 (8) 1.68 (12)	1.68 (8) 1.81 (12)	1.96 (12)
Electronegativity ^b	1.0	0.9	0.8	0.8	0.7
Percent ionic character ^c of bond with O^{2-}	82	83	87	87	89
B. Alkaline earths, elements	Be	Mg	Ca	Sr	Ba
Atomic number	4	12	20	38	56
Naturally occurring isotopes	1	3	6	4	7
Atomic weight (^{12}C)	9.01218	24.305	40.08	87.62	137.33
Electron formula	$[\text{He}]2s^b$	$[\text{Ne}]2s^b$	$[\text{Ar}]2s^b$	$[\text{Kr}]2s^b$	$[\text{Xe}]2s^b$
Ionic radius (Å) and coordination number ^a	0.35 (4)	0.80 (6)	1.08 (6) 1.20 (8)	1.21 (6) 1.33 (8)	1.50 (8) 1.68 (12)
Electronegativity ^b	1.5	1.2	1.0	1.0	0.9
Percent ionic character ^c of bond with O^{2-}	63	71	79	82	84

^a Pauling (1960).

^b Whittacker and Muntus (1970).

^c Electronegativity of oxygen is 3.5.

Table 1.2. Average Rb and Sr concentrations and Rb/Sr ratios of minerals. The number of samples included in the average is stated in parentheses and the range of values is indicated where the information is available

Mineral	Rb (ppm)	Range	Sr (ppm)	Range	Rb/Sr	Reference ^a
A. Silicate minerals in igneous and metamorphic rocks						
Biotite	550 (206)	122 – 2 525	31.1 (378)	0.867 – 676	17.7	1, 19
Muscovite	476 (23)	125 – 1 000	46.0 (139)	2.0 – 398	10.3	1, 10, 23
Phlogopite	–	–	70.7 (8)	3.9 – 180.7	–	1
K-feldspar	561 (144)	53 – 1 650	396 (652)	3 – 5 100	1.42	1, 19, 23
Sanidine	186 (4)	152 – 215	315 (4)	127 – 449	0.590	2
Plagioclase	14.1 (28)	0.14 – 56	566 (440)	0.65 – 5 000	0.0091	1, 19
Amphibole	76.8 (55)	0.2 – 167	106 (186)	3 – 1 060	0.725	1
Kaersutite	5.8 (3)	–	581 (3)	–	0.010	3
Pyroxene	1.28 (27)	0.033 – 3.6	89.1 (222)	3.51 – 853	0.014	1
Clinopyroxene	1.7 (2)	2.3 – 1.1	6.32 (45)	0.226 – 21	0.27	1, 4
Orthopyroxene	0.36 (1)	–	2.02 (1)	–	0.18	4
Olivine	0.13 (11)	0.004 – 0.55	5.51 (30)	0.162 – 21.0	0.024	1
Tourmaline	1.3 (23)	0.1 – 6	601 (23)	38 – 2 469	0.0021	25
Scheelite	0.5 (3)	0.4 – 06	604 (3)	387 – 832	0.00083	25
Actinolite	1.6 (2)	0.8 – 2.3	364 (2)	301 – 426	0.0044	25
Piedmontite (epidote)	0.5 (1)	–	1 150 (1)	–	0.00043	25
Zircon	21 (3)	0.27 – 5.8	50.4 (3)	0.87 – 77.0	0.042	21
Garnet	1.9 (11)	0.019 – 3.9	19.3 (63)	0.98 – 330	0.098	1, 21
Nepheline	85 (8)	50 – 120	209 (8)	80 – 430	0.407	1
Leucite	–	–	482 (5)	110 – 1 400	–	1
Sphene	2.7 (1)	–	1980 (13)	0 – 6 700	0.0014	1, 21
Epidote	31 (4)	4 – 59	8 518 (4)	5 900 – 11 900	0.0036	19
Melliite (carbonatite)	–	–	9 200 (5)	8 400 – 10 900	–	1
Quartz	0.67 (14)	0.001 – 2.5	0.32 (10)	0.03 – 1.0	2.1	2, 6, 11
B. Oxide minerals						
Ilmenite	0.48 (4)	0.15 – 0.76	1.99 (4)	0.21 – 4.57	0.24	24
C. Phosphate minerals						
Apatite (igneous)	1.55 (3)	0.31 – 2.18	1 329 (23)	35 – 73 558	0.0011	1, 21
Apatite (metamorphic)	–	–	2 872 (25)	8 – 9 839	–	1
Apatite (pegmatites)	–	–	483 (18)	4.9 – 4 320	–	1
Apatite (carbonatite)	–	–	6 160 (11)	4 370 – 7 680	–	1, 5
D. Clay minerals						
Glauconite	198 (56)	14 – 283	32.5 (86)	3.8 – 475	6.1	1, 13–16
Kaolinite	47.5 (10)	3.2 – 128.9	44.8 (10)	0.91 – 174.4	1.06	10
Smectite	31.0 (7)	6.01 – 60.8	184.6 (13)	98.1 – 312	0.17	10, 12
Nontronite	56.9 (7)	48.1 – 61.0	472.8 (7)	422 – 499	0.12	20
E. Carbonate minerals						
Calcite (carbonatite)	–	–	2 170 (4)	1 220 – 3 400	–	1
Calcite (travertine)	–	–	923 (92)	20 – 3 900	–	7, 17
Calcite (veins, Archean greenstones)	0.04 (3)	0.02 – 0.06	253 (4)	136 – 600	0.00016	22
Calcite (disseminated, Archean greenst.)	0.58 (2)	0.51 – 0.64	79 (2)	67.6 – 90.0	0.0073	22
F. Miscellaneous						
Fluorite	69.7 (1)	–	539.6 (1)	–	0.129	18
Cryolite	0.1 (2)	0.1 – 0.1	22.0 (2)	5.9 – 38.0	0.0045	18
Sylvite	–	47 – 252	1.0 (0.2)	–	47 – 1 260	1, 9
Carnallite	–	990 – 1 670	1.0 (4)	0.2 – 2.0	495 – 8 350	1, 9
Gypsum and anhydrite	–	–	1 753 (46)	–	–	7, 8

^a References: 1. Wedepohl (1978), 2. Nash and Crecraft (1985), 3. Othman et al. (1990), 4. Stuckless and Irving (1976), 5. Nash (1972), 6. Rossman et al. (1987), 7. Barbieri et al. (1979), 8. Stueber et al. (1984), 9. Braitsch (1971), 10. Clauer (1979), 11. Worden and Compston (1973), 12. Schultz et al. (1989), 13. Grant et al. (1984), 14. Laskowski et al. (1980), 15. Morton and Long (1980), 16. Harris and Fullagar (1991), 17. Demovic et al. (1972), 18. Blaxland (1976), 19. Franklyn et al. (1991), 20. Clauer et al. (1982), 21. Barrie and Shirey (1991), 22. Brooks et al. (1969a), 23. Heller et al. (1985), 24. Burton and O'Nions (1990), 25. Kerrich et al. (1987).

Table 1.11.
Average concentrations of Rb and Sr in plutonic igneous rocks. The number of samples included in the averages is given in parentheses

Rock type	Rb (ppm)	Sr (ppm)	Rb/Sr	SiO ₂ (%)	Ref. ^a
A. Ultramafic rocks					
Dunite	0.39 (9) 0.072–2.42	4.6 (19) 0.12–14.7	0.0085	40.2	1
Pyroxenite	1.65 (3) 0.38–3.47	64 (16) 0.23–199	0.016	50.5	1
Anorthosite	4.5 (18) 1.6–14.7	667 (78) 156–1441	0.0067	54.5	1, 7, 8
Peridotite	1.27 (11) 0.093–4.48	19 (22) 0.4–50.4	0.068	43.5	1
B. Mafic to felsic rocks					
Gabbro	32 (331)	293 (101) 41–860	0.11	48.4	1
Diorite	88 (21)	472 (79) 173–870	0.19	51.9	1
Granodiorite	122 (9)	457 (149) 40–1 100	0.27	66.9	1
Monzonite and quartz monzonite	136	167 (271) 29–876	0.81	69.2	1
Granite	230 (504)	147 (512) 2.16–917	1.56	72.1	1
I type granite	132	253	0.52		9
S type granite	180	139	1.3		9
C. Alkalic rocks					
Alkalic ultramafics (Kola Penin., Russia)	80	1 300	0.062	–	2
Alkali gabbro	–	1 367 (49) 446–2195	–	46.5	1
Nepheline syenite	364 85–950	1098 47–3 500	0.33	55.4	1, 2
Syenite	136 (14)	553 (84) 5.2–2 924	0.25	59.4	1
Lamprophyre	115	1 010	0.11	46.3	5
Kimberlite	68 (39) 63–162	879 (34) 48–1883	0.077	35.0	1, 3, 6
Lamproite	272 (22) 50–614	1 633 (22) 549–3 150	0.18	53.3	5, 6
Carbonatite	–	2 350 (28) 300–3 910	–	–	1
Calciocarbonatite	14 (6) 4–35	7 270 (66) 0–27 820	0.0019	2.72	4
Magnesiocarbonatite	31(4) 2–80	5 830 (29) 507–12 680	0.0053	3.63	4

^a References: 1. Wedepohl (1978), 2. Gerasimovsky (1974), 3. Heinrichs et al. (1980), 4. Woolley and Kempe (1989), 5. Bergman (1987), 6. Fraser et al. (1986), 7. Geist et al. (1990), 8. Kolker et al. (1990), 9. Taylor and McLennan (1985).

Table 1.10. Average distribution coefficients for Rb and Sr in minerals crystallizing from magmas of different composition

Mineral	D(Rb)	Range	D(Sr)	Range	Reference ^a
A. Basalt and andesite					
Olivine	0.0079	0.000179 – 0.011	0.0171	0.000191 – 0.02	1, 2, 3, 28
Orthopyroxene	0.033	0.022 – 0.061	0.012	0.0026 – 0.02	1, 2, 3, 5
Diopside	0.015		0.11	0.078 – 0.12	1, 7, 8
Clinopyroxene	0.029	0.0010 – 0.1	0.13	0.054 – 0.608	2, 3, 5, 9, 10, 11, 12, 28
Augite	0.031		0.12		1
Amphiboles	0.225	0.027 – 0.41	0.605	0.19 – 1.02	2, 5
Hornblende	0.31	0.29 – 0.33	0.47	0.46 – 0.48	1, 11
Plagioclase	0.099	0.0262 – 0.50	1.89	1.18 – 3.06	1, 2, 10, 11, 13, 14, 28
Mica	3.2		0.21		5
Phlogopite	3.08		0.08		1, 2
Garnet	0.042		0.012		1
Apatite	–		5.05	3.7 – 6.4	5
Whitlockite	–		1.00 (1)		15
Perovskite	–		0.734		27
B. Dacite and rhyolite					
Orthopyroxene	0.09	0.0005 – 0.29	0.030	0.009 – 0.05	2
Hypersthene	0.0027		0.085		1
Clinopyroxene	0.061	0.032 – 0.09	0.516		1, 2
Hornblende	0.014		0.022		1
Plagioclase	0.070	0.024 – 0.46	9.1	1.5 – 40	1, 2, 16, 17, 18, 19
Alkali feldspar	0.58	0.11 – 1.04	5.45	2.7 – 26	1, 2, 17, 20
Sanidine	0.70	0.28 – 2.4	4.7	2 – 7.3	16, 19, 21, 22
Quartz	0.014	0.012 – 0.016	–		16
Garnet	0.0087	0.0085 – 0.009	0.017	0.015 – 0.02	1, 2
Biotite	3.21	2.24 – 5.3	0.21	0.08 – 0.53	1, 2, 16, 17, 21
Muscovite	1.54		0.104		17
C. Alkalic rocks					
Olivine	0.045	0.02 – 0.08	0.012	0.003 – 0.02	4, 6, 23
Orthopyroxene	0.022		0.017		6
Clinopyroxene	0.049	0.004 – 0.04	0.14	0.08 – 0.16	4, 6, 23, 24
Magnetite	0.35	0.14 – 0.47	0.69	0.68 – 0.70	6, 23, 24
Amphibole	0.11	0.09 – 0.14	–		6
Hornblende	1.9		0.3		23
Kaersutite	0.2		0.61		4
Plagioclase	0.16	0.03 – 0.39	3.1	1 – 5	6, 24, 25
Alkali feldspar	0.3		10		23
Sanidine	0.21	0.16 – 0.25	1.5	0.9 – 2.8	6, 21, 25
Anorthoclase	0.15	0.11 – 0.18	4.9	2.82 – 30	24, 25, 26
Melilite (Ak 12 to 90)	–		0.84	0.62 – 1.12	8, 27
Biotite	2.6	1.9 – 3.2	0.46	0.21 – 0.7	4, 23
Apatite	–		2.4	1 – 5	4, 24
D. Undifferentiated					
Plagioclase	0.069	0.0294 – 0.188	1.78	1.27 – 2.84	29
K-feldspar	0.659		3.87		29
Clinopyroxene	0.0497	0.0129 – 0.284	0.166	0.00187 – 0.516	29
Orthopyroxene	0.0217	0.0148 – 0.0287	0.0172	0.0104 – 0.0241	29
Micas	2.418	0.936 – 3.26	0.291	0.0812 – 0.672	29
Hornblende	0.294	0.0448 – 0.427	0.459	0.188 – 0.641	29
Garnet	0.00851		0.0154		29
Olivine	0.00984	0.00839 – 0.0113	0.0139	0.00937 – 0.0185	29

^a References: 1. Arth and Hanson (1975), 2. Henderson (1982), 3. Shimizu et al. (1982), 4. Irving and Price (1981), 5. Irving and Frey (1984), 6. LeMarchand et al. (1987), 7. Grutzeck et al. (1974), 8. Kuehner et al. (1989), 9. Shimizu (1974), 10. Sun et al. (1974), 11. Dostal et al. (1983a), 12. Ray et al. (1983), 13. Warren (1983), 14. Drake and Weill (1975), 15. Irving (1978), 16. Nash and Crecraft (1985), 17. Mittlefehldt and Miller (1983), 18. Dupuy (1972), 19. Stix and Gorton (1990), 20. Long (1978), 21. Mahood and Hildreth (1983), 22. Leeman and Phelps (1981), 23. Villemant et al. (1981), 24. McDonough and Nelson (1984), 25. Berlin and Henderson (1969), 26. Mahood and Stimac (1990), 27. Nagasawa et al. (1980), 28. Hart and Brooks (1974), 29. Philpotts and Schnetzler (1970).

Fig. 1.10.

a Average Rb and Sr concentrations of mafic to felsic plutonic igneous rocks with increasing degree of magmatic differentiation represented by increasing SiO_2 concentrations; **b** The Rb/Sr ratio initially increased slowly during magmatic differentiation until Sr has been removed from the magma by crystallization of feldspars (Source: data from Table 1.10)

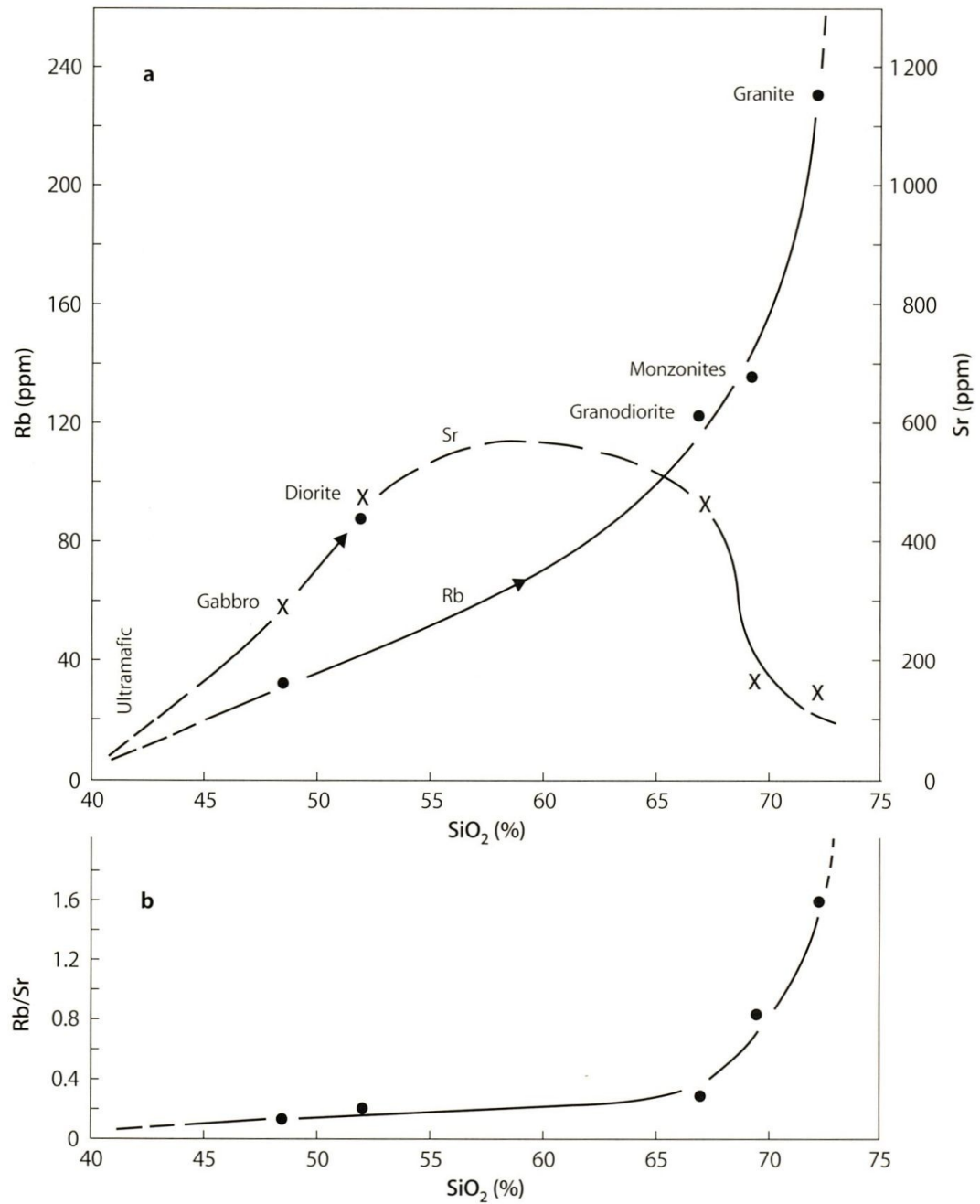


Table 1.4. Abundances of the isotopes of Sr in seawater ($^{87}\text{Sr}/^{86}\text{Sr} = 0.70916$)

Ratio	Value	Isotope	Abundance (% by number)
$^{84}\text{Sr}/^{88}\text{Sr}$	0.006756 ^a	^{84}Sr	0.5579
$^{86}\text{Sr}/^{88}\text{Sr}$	0.119400	^{86}Sr	9.8610
$^{87}\text{Sr}/^{88}\text{Sr}$	0.084673 ^b	^{87}Sr	6.9929
$^{88}\text{Sr}/^{88}\text{Sr}$	1.000000	^{88}Sr	82.5880
Sum	1.210829		99.9998

^a $^{84}\text{Sr}/^{88}\text{Sr} = (^{84}\text{Sr}/^{86}\text{Sr}) \times (^{86}\text{Sr}/^{88}\text{Sr})$.

^b $^{87}\text{Sr}/^{88}\text{Sr} = (^{86}\text{Sr}/^{88}\text{Sr}) \times (^{87}\text{Sr}/^{86}\text{Sr})$.

Table 1.3. Isotopic abundances of ^{85}Rb and ^{87}Rb for the value of 2.59265 which is recommended by the Subcommission on Geochronology of the International Union of Geological Sciences (Steiger and Jäger 1977)

Ratio	Value	Isotope	Abundance (% by number)
$^{85}\text{Rb}/^{87}\text{Rb}$	2.59265	^{85}Rb	72.1654
$^{87}\text{Rb}/^{87}\text{Rb}$	1.00000	^{87}Rb	27.8346
Sum	3.59265		100.0000

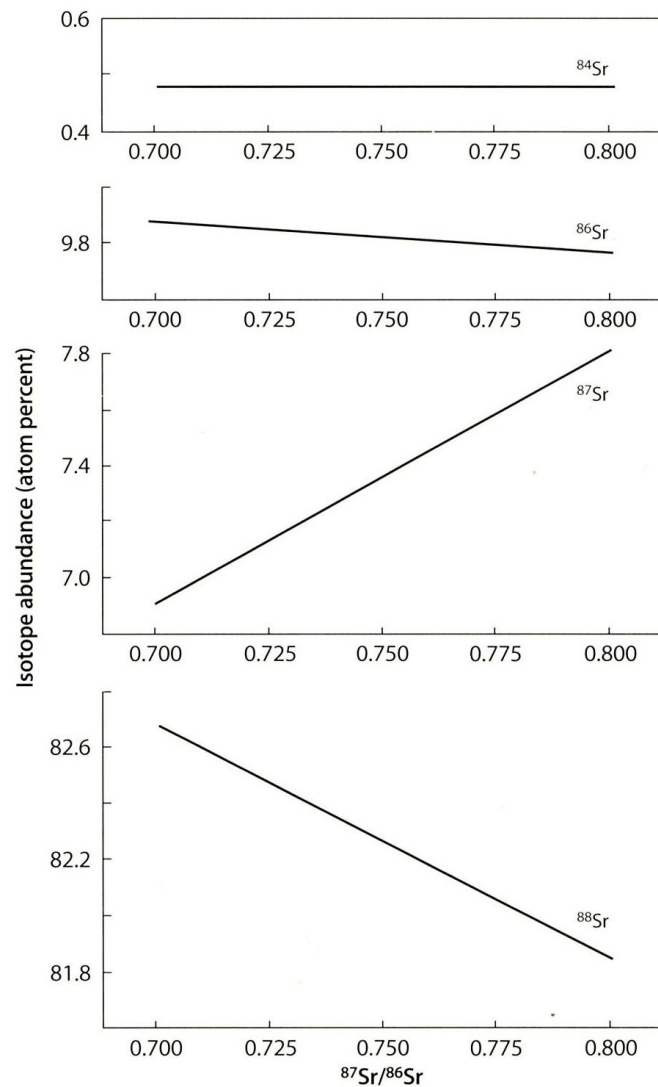
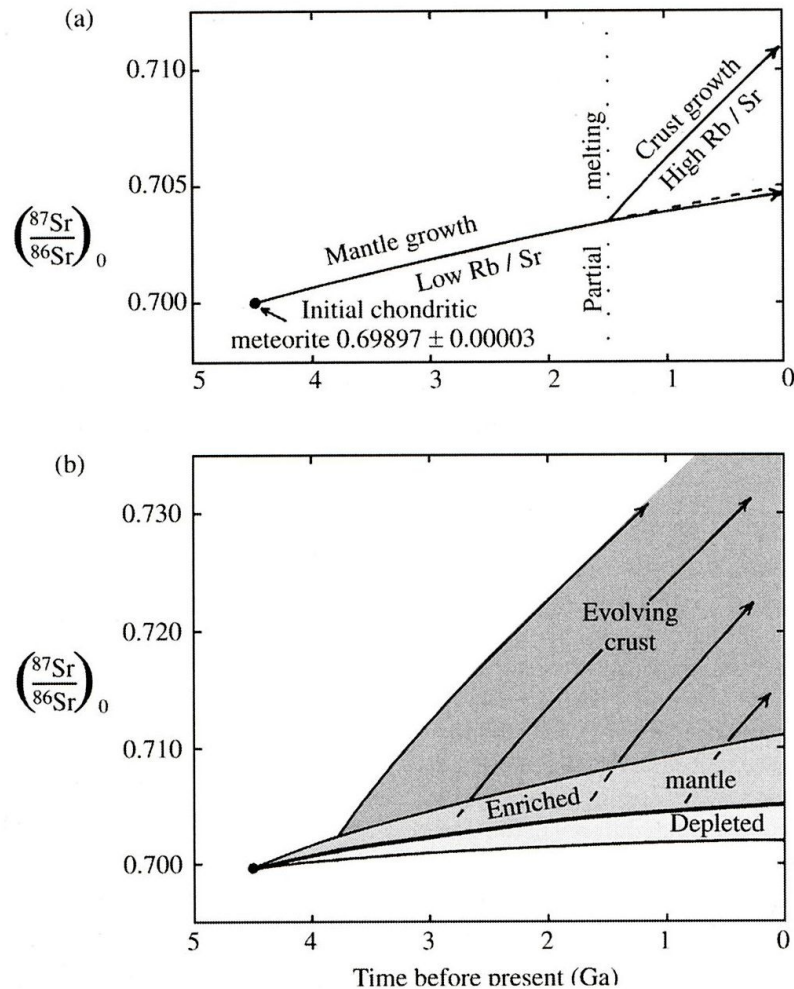


Fig. 1.1. Changes of the abundances (in percent by number of atoms) of the naturally-occurring isotopes of Sr with increasing abundance of radiogenic ^{87}Sr expressed as the atomic $^{87}\text{Sr}/^{86}\text{Sr}$ ratio. Even though the abundances of the non-radiogenic isotopes (^{84}Sr , ^{86}Sr , and ^{88}Sr) decrease with increasing $^{87}\text{Sr}/^{86}\text{Sr}$, the number of these isotopes in a unit weight of sample remains constant



2.26 Schematic strontium isotope evolution diagrams for the Earth. Filled circle represents an assumed parental chondritic meteorite whose initial $(^{87}\text{Sr}/^{86}\text{Sr})_0$ ratio at 4.5 Ga, when the Earth accreted from primordial material, was 0.69897 ± 0.00003 . Note that growth lines are slightly curved because the amount of ^{87}Rb decaying to ^{87}Sr decreases through time. (a) Single-stage model with hypothetical partial melting event at 1.5 Ga. Thereafter, mantle growth is at a slightly lower rate because of extracted Rb from a depleted mantle. (b) Multistage model in which the mantle has been partially melted many times throughout its history to create a growing, evolving crust. Metasomatic processes create an incompatible-element-*enriched* mantle (Section 11.2.2); other parts of mantle are relatively *depleted* through partial melting processes.

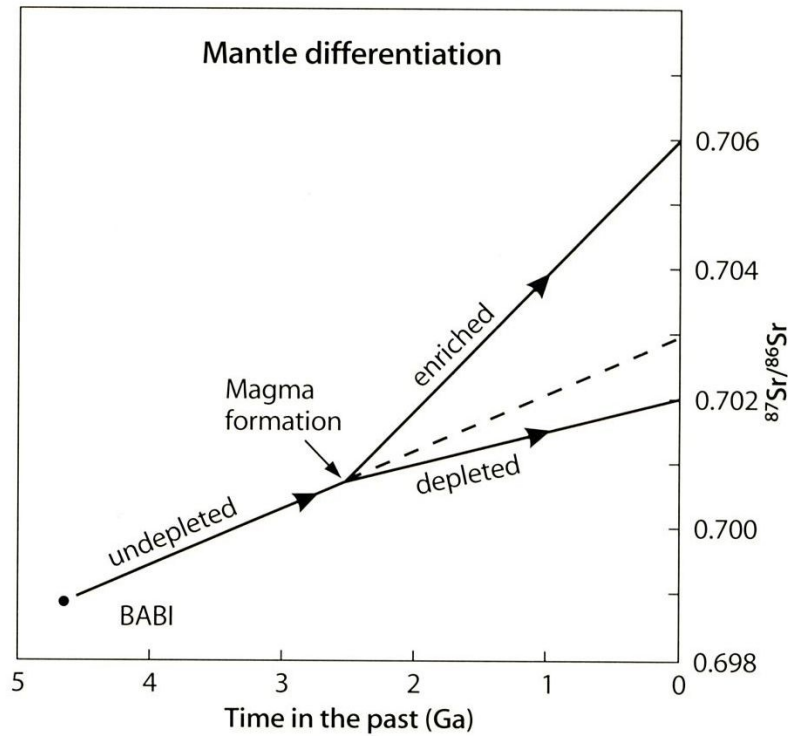


Fig. 2.1. Schematic diagram illustrating the isotope evolution of Sr in a small volume of rock in the upper mantle before and after formation of magma by partial melting. The $^{87}\text{Sr}/^{86}\text{Sr}$ ratio of a parcel of undepleted rocks in the upper mantle increases initially from 0.699 (Basaltic Achondrite Best Initial) at 4.55 Ga to 0.7008 at 2.5 Ga when magma forms by partial melting. Since the Rb/Sr ratio of the residual solids is less than that of the silicate liquid, the $^{87}\text{Sr}/^{86}\text{Sr}$ ratio of the residual solids (*depleted* mantle) subsequently increases more slowly than it did before melting occurred. The present value of the $^{87}\text{Sr}/^{86}\text{Sr}$ ratio in the *depleted* region of the upper mantle in the illustration is 0.7020. If the *enriched* silicate liquid in this illustration crystallized without assimilating Sr from the continental crust, its $^{87}\text{Sr}/^{86}\text{Sr}$ ratio at the present time is 0.7060. If the undepleted mantle rocks had remained undisturbed, their present $^{87}\text{Sr}/^{86}\text{Sr}$ ratio is 0.7030

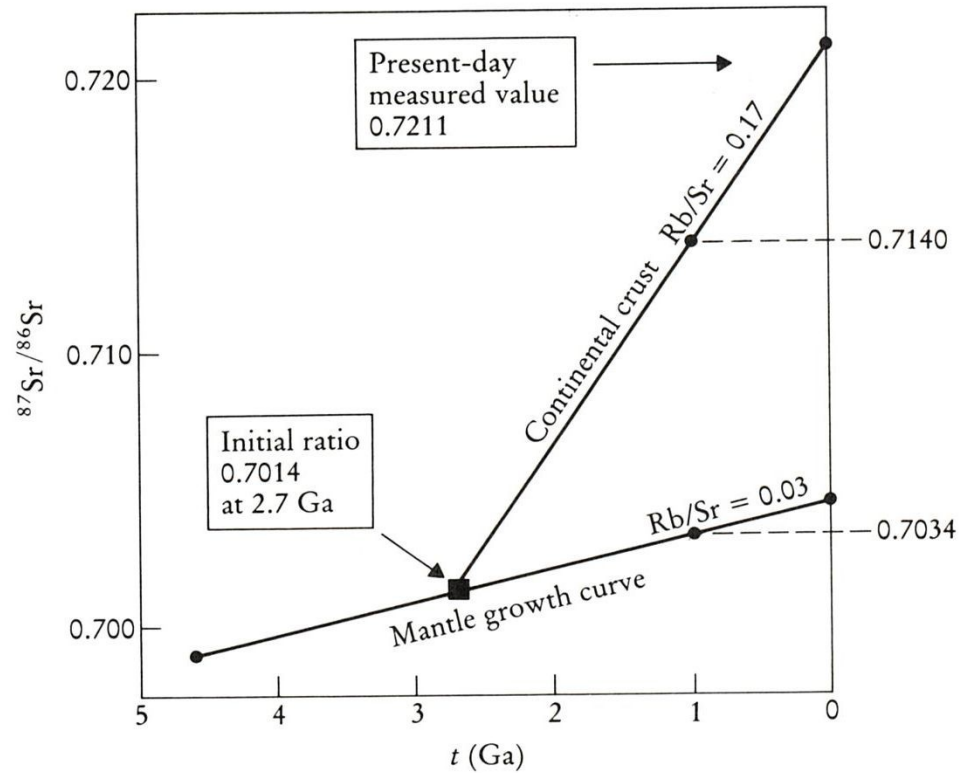


Figure 6.15 The evolution of $^{87}\text{Sr}/^{86}\text{Sr}$ with time in the continental crust and mantle. At 2.7 Ga mantle differentiation led to the formation of new continental crust. The new crust inherited an initial $^{87}\text{Sr}/^{86}\text{Sr}$ ratio of 0.7014 from its parent mantle but acquired a substantially different Rb/Sr ratio (0.17) compared with 0.03 in the mantle. The higher Rb/Sr ratio in the continental crust led to an accelerated growth of $^{87}\text{Sr}/^{86}\text{Sr}$ with time in the continental crust relative to that in the mantle so that the present-day measured value in the crust is 0.7211 compared with 0.7045 in the mantle. The $^{87}\text{Sr}/^{86}\text{Sr}$ ratios shown on the right-hand side of the diagram indicate the initial ratios in melts formed from continental crust at 1.0 Ga (0.7140) and from the mantle at 1.0 Ga (0.7034).

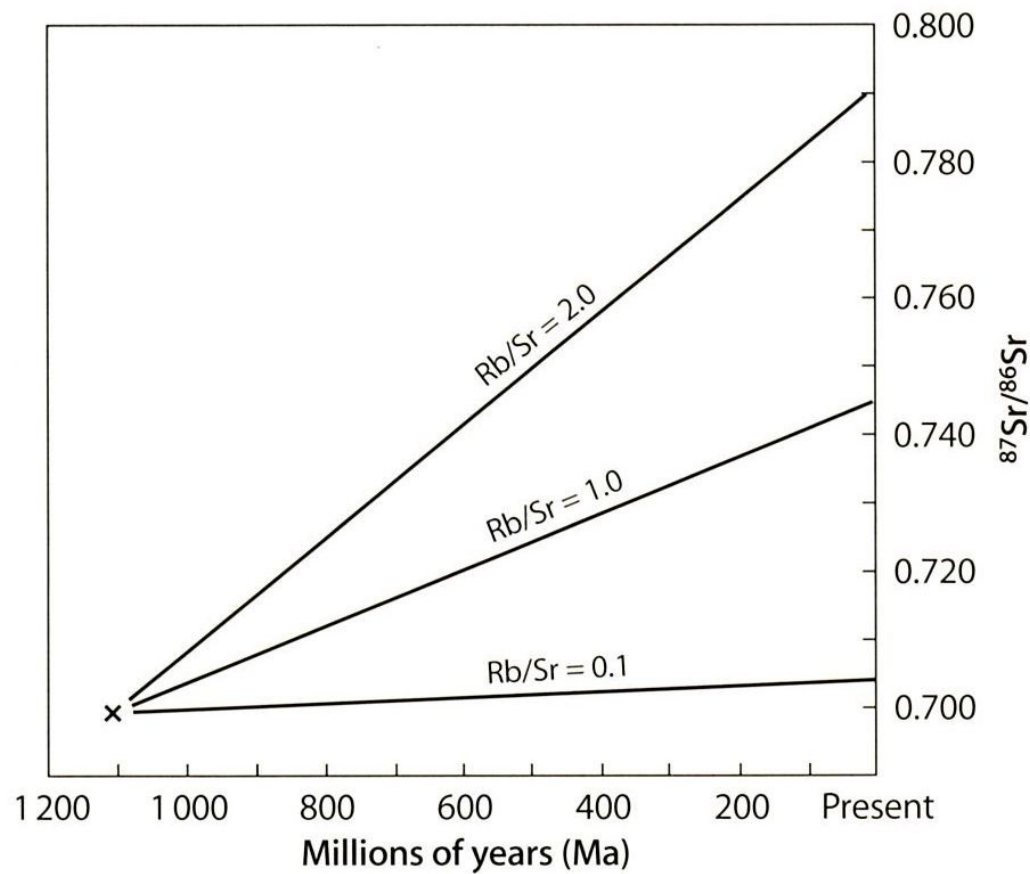


Fig. 1.2. Time-dependent evolution of the isotope composition of Sr in systems having different Rb/Sr ratios. The diagram illustrates the increase of the $^{87}\text{Sr}/^{86}\text{Sr}$ ratios of specimens of comagmatic rocks that crystallized at 1100 million years (Ma) from a homogeneous magma whose $^{87}\text{Sr}/^{86}\text{Sr}$ ratio was 0.700. The present $^{87}\text{Sr}/^{86}\text{Sr}$ ratios and Rb/Sr ratios of these rock specimens can be used to determine the coordinates of the point of convergence. In the simple case under consideration, the coordinates are the $^{87}\text{Sr}/^{86}\text{Sr}$ of the Sr in the magma (initial $^{87}\text{Sr}/^{86}\text{Sr}$) and the time elapsed since crystallization of the magma, i.e. the *age* of the rocks (based on Eq. 1.16)

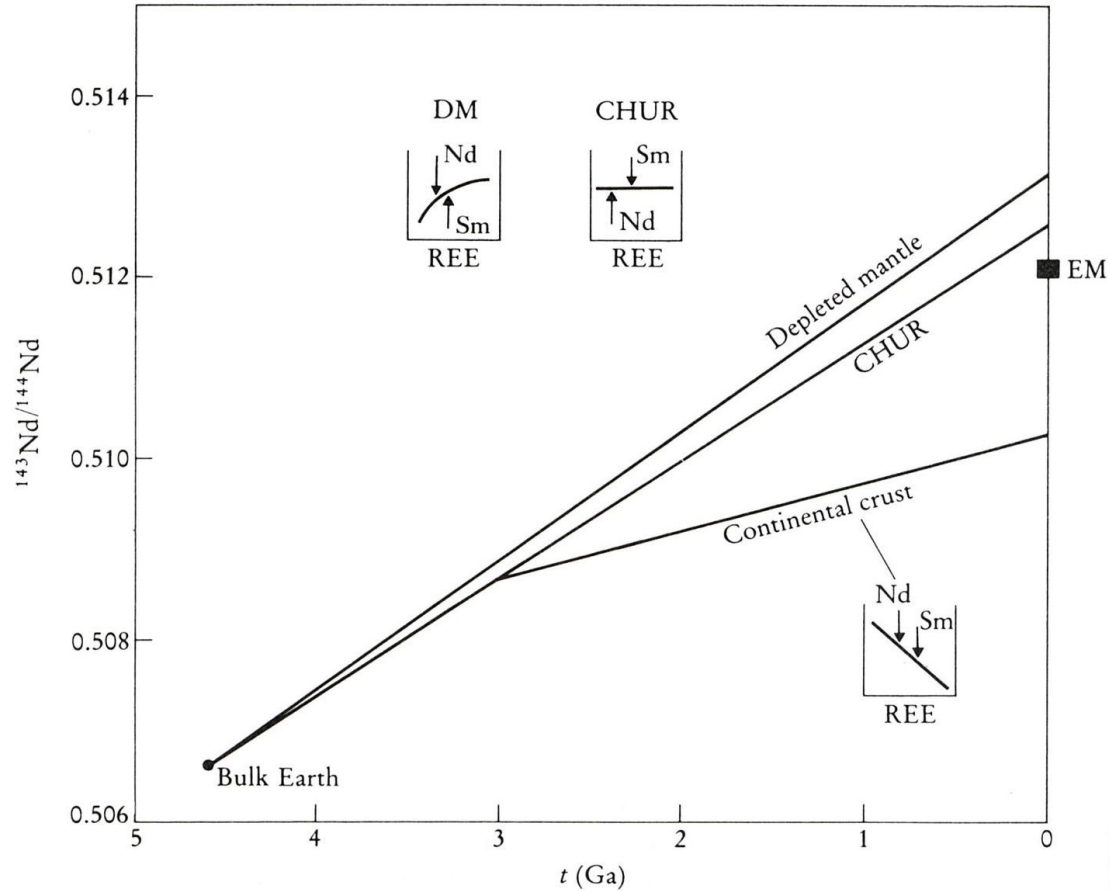
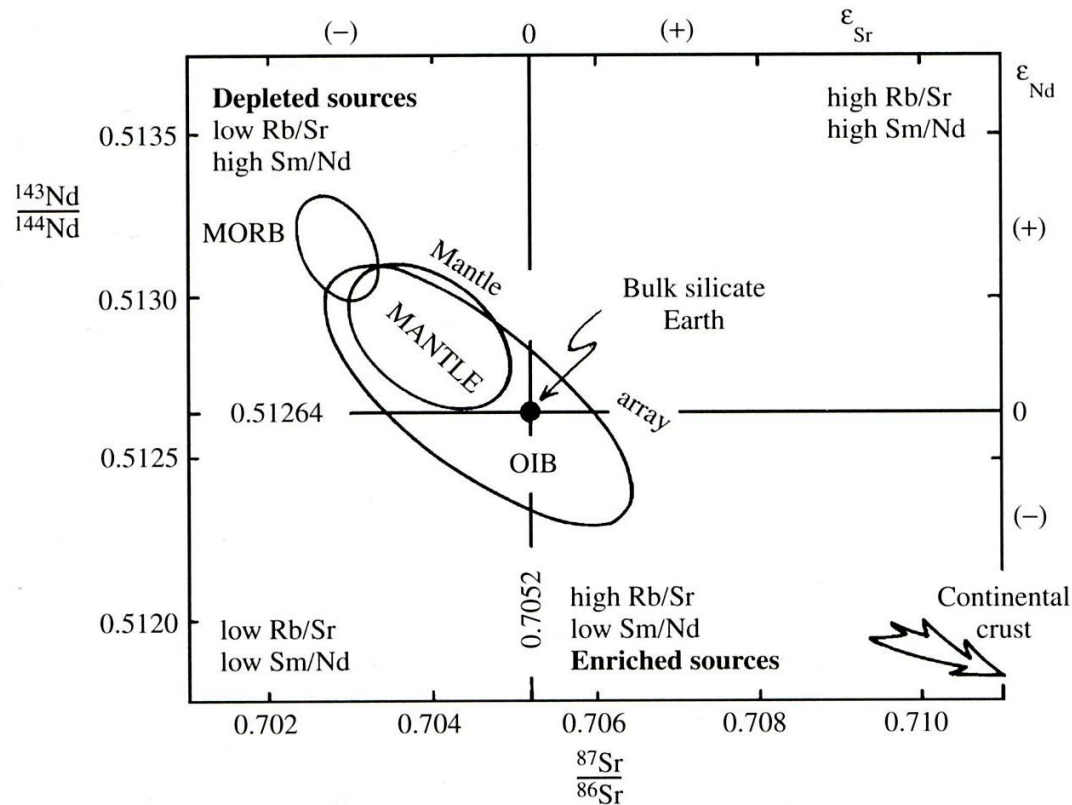


Figure 6.16 The evolution of $^{143}\text{Nd}/^{144}\text{Nd}$ isotopes with time in the mantle, the continental crust and the bulk Earth. Relative to the bulk Earth (CHUR) in which the fractionation of Sm/Nd is normalized to unity, the depleted mantle (DM) has a high Sm/Nd ratio and shows higher $^{143}\text{Nd}/^{144}\text{Nd}$. The continental crust has lower Sm/Nd and shows a retarded $^{143}\text{Nd}/^{144}\text{Nd}$ evolution with time. Enriched mantle (EM) shows some affinity with the continental crust inasmuch as it also has a retarded $^{143}\text{Nd}/^{144}\text{Nd}$ evolution. Note that in the Sm–Nd system the crust shows retarded isotopic evolution whilst in the Rb–Sr system it shows accelerated evolution relative to the bulk Earth and mantle (cf. Figure 6.15).



2.27 Sr and Nd isotope ratio correlations. All terrestrial rocks are derived from a **primordial bulk silicate Earth**. The mantle array is defined by relatively depleted, mantle-derived, mid-ocean ridge basalt (MORB) and more enriched ocean island basalt (OIB), as well as fragments (xenoliths) of the suboceanic mantle (labeled MANTLE) brought up in erupted OIBs. Continental rocks plot well off the diagram to the lower right. The ϵ_{Sr} and ϵ_{Nd} notation refers to the difference between the measured $^{87}Sr/^{86}Sr$ and $^{143}Nd/^{144}Nd$ ratios in rock samples and the reference bulk Earth ratio (for further details see Rollinson, 1993). (Redrawn from Rollinson, 1993.)

Radiogenic isotopes in petrogenesis

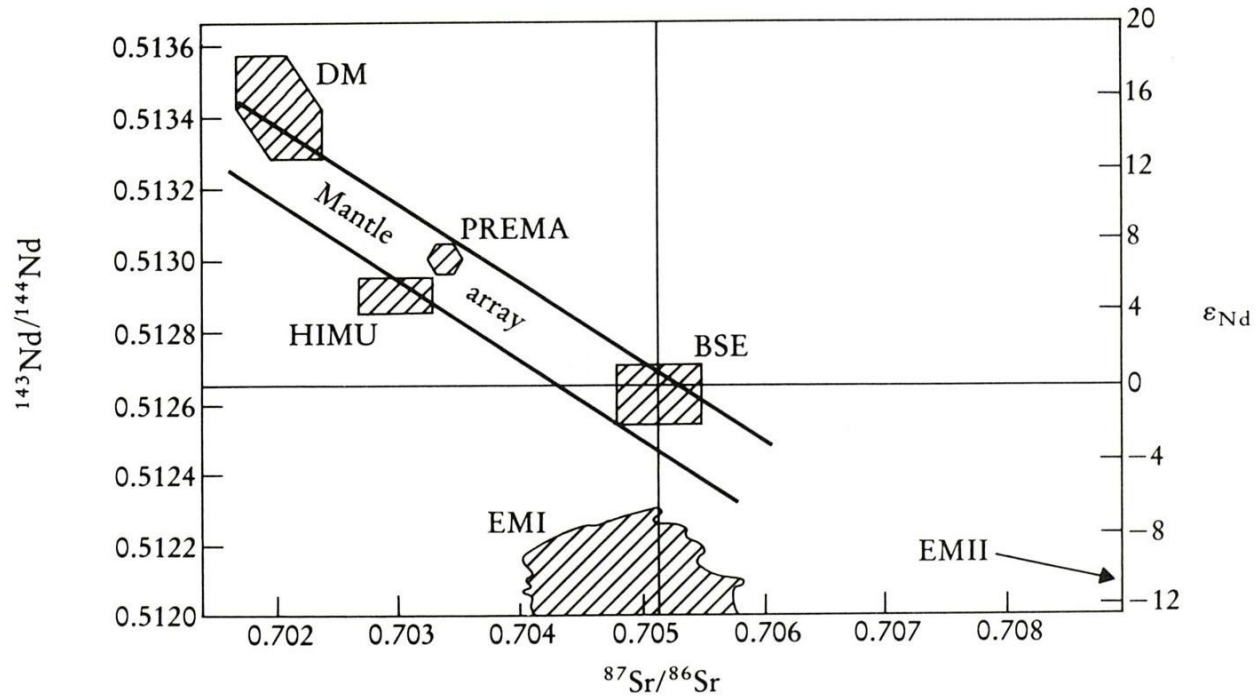


Figure 6.9 $^{143}\text{Nd}/^{144}\text{Nd}$ vs $^{87}\text{Sr}/^{86}\text{Sr}$ isotope correlation diagram, showing the main oceanic mantle reservoirs of Zindler and Hart (1986). DM, depleted mantle; BE, bulk silicate Earth; EMI and EMII, enriched mantle; HIMU, mantle with high U/Pb ratio; PREMA, frequently observed PREvalent MANTle composition. The Mantle array is defined by many oceanic basalts and a bulk Earth value for $^{87}\text{Sr}/^{86}\text{Sr}$ can be obtained from this trend.

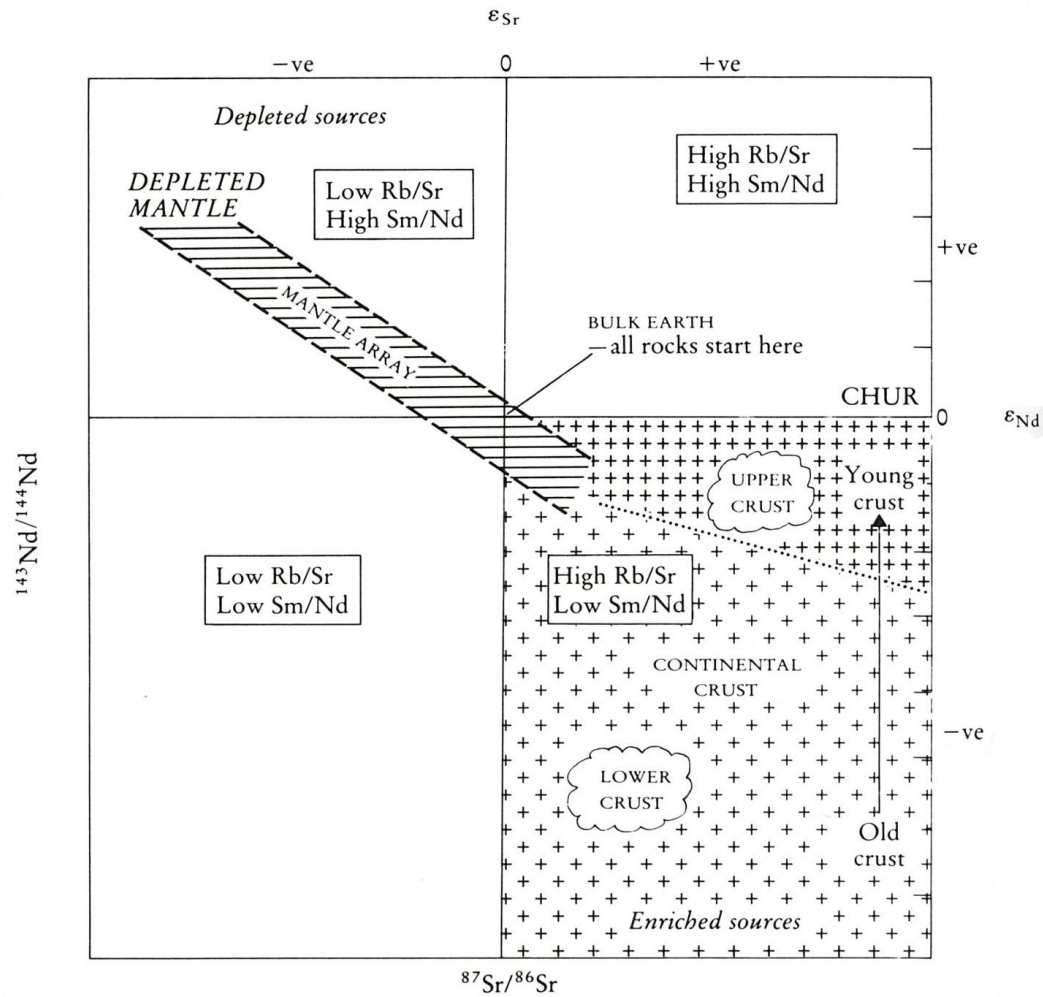
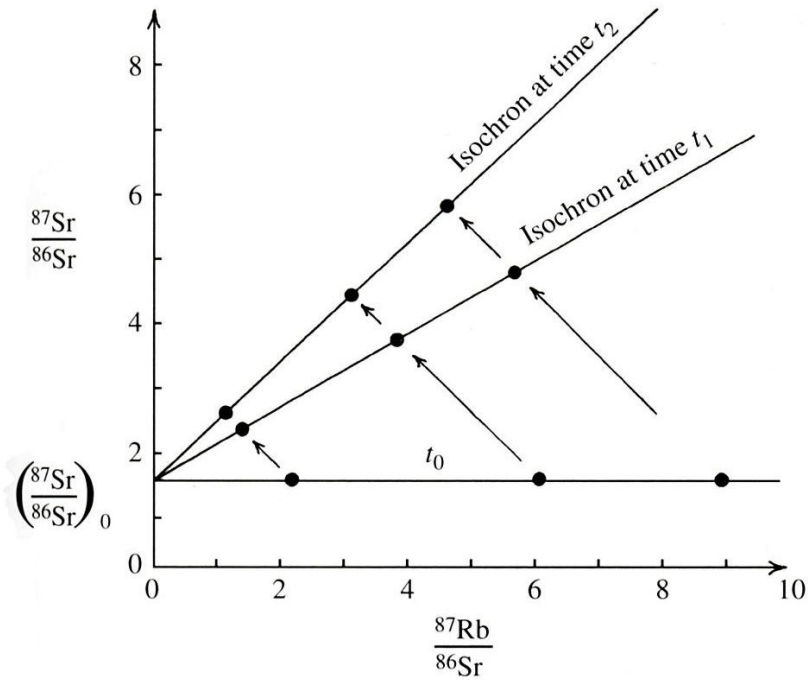


Figure 6.10 $^{143}\text{Nd}/^{144}\text{Nd}$ vs $^{87}\text{Sr}/^{86}\text{Sr}$ (ϵ_{Nd} vs ϵ_{Sr}) isotope correlation diagram showing the relative positions of depleted and enriched mantle sources. Most non-enriched mantle reservoirs plot in the upper left 'depleted' quadrant (cf. Figure 6.9) whereas most crustal rocks plot in the lower right 'enriched' quadrant. Upper and lower crust tend to plot in different positions in the crustal quadrant (from DePaolo and Wasserburg, 1979)



2.25 Schematic Rb-Sr **isochron** diagram for comagmatic rocks or minerals decaying through time. Three samples of rocks or minerals (solid circles) having identical initial $(^{87}\text{Sr}/^{86}\text{Sr})_0$ ratios crystallized at the same time, t_0 , from a magma or related magma, after which the isotopic system remained closed. The initial $^{87}\text{Rb}/^{86}\text{Sr}$ ratios of the three samples differed because of different Rb/Sr ratios; muscovite, for example, would have a greater ratio than plagioclase. Subsequent to time t_0 , individual rocks or minerals track along straight lines having a slope of -1 due to decay of ^{87}Rb to ^{87}Sr . At any one time, such as t_1 , and so on, points representing the analyzed samples define a straight line isochron whose positive slope is dictated by the age of the system since crystallization occurred to close it.

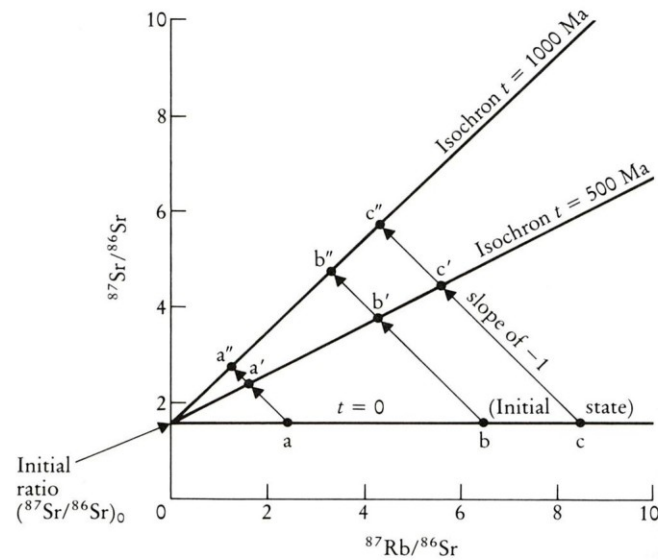


Figure 6.1 A schematic isochron diagram showing the evolution of a suite of igneous rocks (a, b, c) over 500 Ma and 1000 Ma. The samples formed at $t = 0$ from the same batch of magma which subsequently differentiated. At $t = 0$ each member of the rock suite has the same initial ratio $(^{87}\text{Sr}/^{86}\text{Sr})_0$ but because the magma suite is chemically differentiated each rock has a different concentration of Rb and Sr and so a different $^{87}\text{Rb}/^{86}\text{Sr}$ ratio. Each sample plots as a separate point on the $^{87}\text{Rb}/^{86}\text{Sr}$ vs $^{87}\text{Sr}/^{86}\text{Sr}$ isochron diagram. From $t = 0$ to $t = 500$ Ma or $t = 1000$ Ma individual samples evolve along a straight line with a slope of -1 (for example $a \rightarrow a' \rightarrow a''$), reflecting the decay of a single atom of ^{87}Rb to a single atom of ^{87}Sr . [In practice the resulting change in $^{87}\text{Sr}/^{86}\text{Sr}$ is small and so the vertical scale is normally exaggerated and the path taken by points is therefore much closer to a vertical line.] The amount of ^{87}Sr produced in a given sample is proportional to the amount of ^{87}Rb present. The slopes of the isochrons ($t = 500$ Ma, $t = 1000$ Ma) are proportional to the ages of the sample suite. The intercept on $^{87}\text{Sr}/^{86}\text{Sr}$ is the initial ratio.

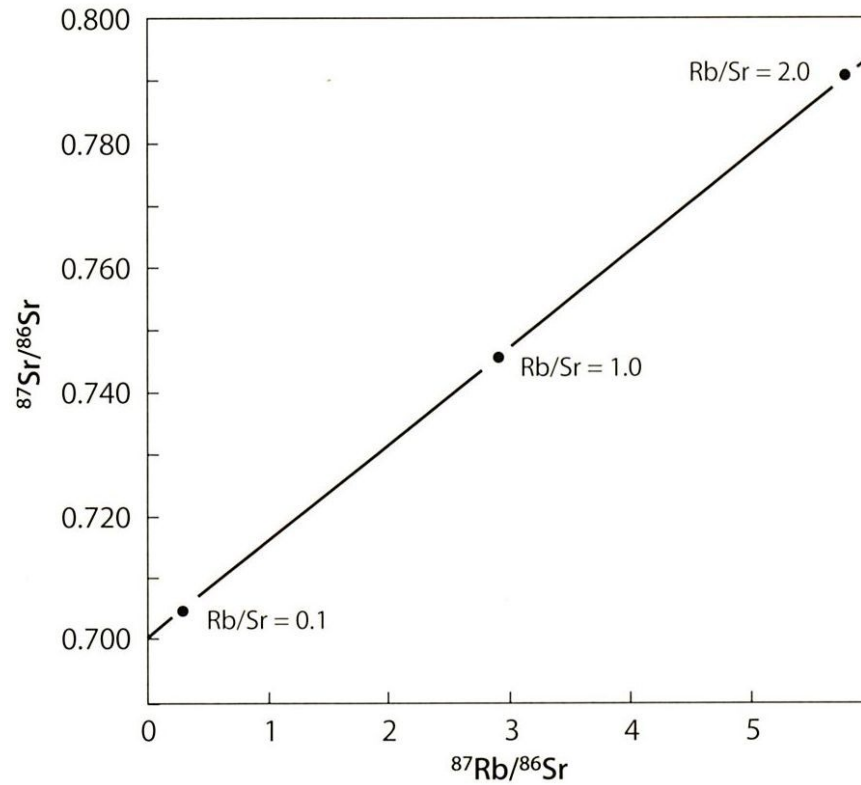


Fig. 1.3. Rb-Sr isochron formed by three whole-rock specimens of igneous rocks that crystallized from the same magma at the time. Rock samples that satisfy these conditions lie along a straight-line isochron in accordance with Eq. 1.12. The slope of the isochron yields the age of the rocks by Eq. 1.18 and the intercept on the vertical axis is the $^{87}\text{Sr}/^{86}\text{Sr}$ ratio of the magma at the time the rock samples crystallized from it. The three data points used to draw the isochron in this diagram are identical to the rock samples used in Fig. 1.2 to illustrate the evolution of the isotope composition of Sr